EUROPEAN ORGANIZATION FOR NUCLEAR RESEARCH

CERN – SL DIVISION

SL-Note-2000-005 MS

Calculation of harmonic coefficients of the LEP Spectrometer Magnet

M. Sassowsky

Abstract

The LEP spectrometer aims at a precision measurement of the LEP beam energy. One of the key elements is the magnet that bends the beam. This note describes the determination of local and integrated harmonic coefficients from a three dimensional field model of the magnet.

Geneva, Switzerland

November 22, 1999

Contents

List of Figures

1 Abstract

The LEP spectrometer [1] aims at a precision measurement of the LEP beam energy. One of the key elements is the magnet that bends the beam. This note describes the determination of local and integrated harmonic coefficients from a three dimensional field model of the magnet.

2 Introduction

The aim of the LEP spectrometer project [1] is the precise measurement of the LEP beam energy. The basic measurement principle consists in bending the particle beam by a dipole magnet of bending power $\int B\,dl$. A beam of momentum p is deflected by the angle Θ:

$$\Theta = k \cdot \frac{\int B\,dl}{p} \qquad\qquad k = 0.2998\,\frac{\text{GeV/c}}{\text{Tm}} \tag{2.1}$$

As the spectrometer magnet is installed in the LEP accelerator, the bend angle is fixed and given by the machine layout. Measuring at different energies thus implies that the relative change of $\int B\,dl$ as a function of the beam energy must be known precisely.

The LEP spectrometer magnet is a modified version of the MBI magnets [4] [5] installed in the injection region. It is a C-magnet, the coil design is close to a racetrack shape.

The magnetic field calculations carried out to predict some of the magnetic properties of the spectrometer magnet are described in [2]. The three dimensional model described there has been extended to a full length model. The transverse field homogeneity of the two dimensional model described in [2] is reproduced by the improved three dimensional model.

3 Multipole expansion of the magnetic field

Throughout this note the coordinate system shown below in Fig. 1 is adopted. z is the longitudinal direction, $z = 0$ corresponds to the magnet centre and $z = \pm 2875$ mm corresponds to the end of the yoke. x is the transverse direction; $x = 0$ mm is the nominal centre of the aperture, i.e. the nominal transverse beam position. y is the vertical direction, $y = 0$ is in the symmetry plane of the magnet.

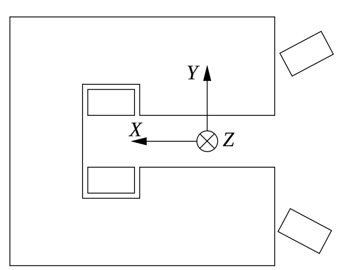

Figure 1: Coordinate system

The magnetic field inside an accelerator magnet, sufficiently far from the extremities, is two dimensional and has no z component. It can be written as a multipole expansion:

$$B(z) \;=\; \sum_{n=1}^{\infty} C_n e^{-in\alpha_n} \left(\frac{z}{r_0}\right)^{n-1} \tag{3.1}$$

$$
\begin{aligned}
z &= x + iy \\
B(z) &= B_y + iB_x
\end{aligned}
$$

C_n and α_n are the harmonic coefficients; C_n are the amplitudes and α_n the phases. r_0 is the reference radius. For a pure dipolar field of strength B, pointing in y direction, this expansion reduces to:

$$
\begin{aligned}
C_1 &= B,\ \alpha_1 = 0 \\
B_y &= B \\
B_x &= 0
\end{aligned}
$$

For a real magnet the finite size of the poles leads to a transverse inhomogeneity and therefore to higher order harmonics. In the case of a symmetric dipole, the harmonics are constrained to $n = 1, 3, 5, \ldots$. Defects of the magnet such as asymmetries, mechanical imperfections or inhomogeneities of the magnetic properties of the steel can create harmonics of any order.

The finite mesh size of a finite element model can produce fake harmonics. A reduction of such fake harmonics ap ears to be possible by adapting the mesh to the circular path for the harmonic analysis. However for the results presented in this note, this was not done; the mesh in the center of the aperture is strictly rectangular.

The multipole expansion 3.1 is only valid sufficiently far from the ends of the magnet yoke. In the end regions, the field has not only x and y components, but an additional z component. The three degrees of freedom cannot be described by only two parameters (C_n, α_n) per order.

However it can be shown that the integral field essentially behaves as a two dimensional field provided that the integration is carried out over an appropriate region [3]. The endpoints of the integration region have to be chosen so that the z component of the field vanishes, i.e. either well inside the magnet yoke or sufficiently far outside the magnet.

Therefore the integrated harmonic coefficients are determined for three regions: the central field ($|z| \leq 2675$ mm), the end field (2675 mm $< |z| \leq 3600$ mm) and the total field ($|z| \leq 3600$ mm).

The finite element program Opera3D [6] [7] [8] that was used for the field model does not permit the calculation of integrated harmonics in a single command, so a dedicated command script was used. For each harmonic analysis, the field is integrated n_p times parallel to the z axis from z_{min} to z_{max} using the $LINE command. The x and y coordinates lie equally spaced on a circle with radius r_0 and center coordinates (x_{cen}, y_{cen}). The field integrals are stored in temporary variables and the harmonic coefficients are calculated by Fourier transformation. The number of points n_p should be chosen at least by a factor two higher than the highest order to be analysed (Nyquist theorem). For the results presented in this note, $n_p = 64$ was chosen to be safely above this limit.

In an inhomogeneous field the calculated harmonic coefficients obviously depend on the position (x_{cen}, y_{cen}) of the reference axis as well as on the reference radius.

4 Results

4.1 Scaling of harmonic amplitudes with reference radius

If the reference radius r_0 in Eq. 3.1 is scaled by a factor k to a different value $r_0' = k \cdot r_0$, the harmonic amplitudes are scaled by a factor k^{n-1}. Thus $\sqrt[n-1]{C_n}$ should be proportional to r_0. The expected behaviour is found for the quadrupolar and sextupolar component for reference radii between 5 and 45 mm, see Fig. 2 in the Appendix. For the higher orders the harmonic amplitudes are over-estimated at small reference radii (≤ 20 mm). The probable reason is that the mesh size gets too large compared to the analysed region and the higher orders requiring adequate ”sampling” of the field are not resolved properly (Opera3D interpolates linearly between mesh points).

The harmonics shown in Fig. 2 are the ones obtained from the central field; a similar behaviour is found for the end field and total field harmonics.

For the results shown in the following subchapters, a reference radius $r_0 = 30$ mm was used.

4.2 Transverse homogeneity from harmonics

To test the numerical precision of the harmonic coefficients, they are converted back to a homogeneity curve using Eq. 3.1. This curve is compared to the homogeneity curve obtained directly from the field model. Fig. 3 shows the comparison for a reference radius $r_0 = 30$ mm and the reference axis for the harmonic analysis at $(x_{cen}, y_{cen}) = (0, 0)$. The points are obtained directly from the field model, the line represents the homogeneity curve as obtained from the harmonics. The three lefthand plots correspond to the homogeneity as a function of x at $y = 0$, the three righthand plots to the homogeneity as a function of y at $x = 0$. In general good agreement is found, even for values of x and y larger then r_0. The worst discrepancy is about 10 ppm for the homogeneity of the end field as a function of y around $|y| = 35$ mm. Note that this discrepancy is tiny compared to the actual field errors caused by the limited mechanical accuracy and the spread in the magnetic properties of the steel. All harmonics up to $n = 6$ have been used and are significant.

Fig. 4 shows the same comparison, but for a field level equivalent to an energy of 44 GeV instead of 100 GeV.

4.3 Harmonic spectra

Figs. 5 and 6 show the harmonic spectra at 100 GeV and 44 GeV. The amplitudes are given in units, i.e. normalised to $10^{-4} \cdot C_1$. The phase angles $n\alpha_n$ are given in degrees relative to the phase angle of the dipole component.

For the central field all harmonic amplitudes at 100 GeV are below one unit, for the integral field all amplitudes are below 0.3 units. The phases are either close to 0^o or 180^o relative to the dipole component. For the harmonics 2 to 5 a phase difference of 180^o between the central field and the end field can be seen. This leads to a partial cancellation of the hamonics so that the amplitudes of the total field are reduced with respect to the central field. The main difference between the spectra at 100 Gev and 44 GeV is the different phase of the quadrupolar component of the total field (180^o at 100 GeV, 0^o at 44 GeV). This corresponds to the fact that the homogeneity curves of the integrated field have slopes of opposite sign at the two field levels (negative at 100 GeV, positive at 44 GeV). The amplitude of the quadrupolar component is slightly lower at 44 GeV than at 100 GeV.

4.4 Transverse displacement of reference axis

In an inhomogeneous field the calculated harmonic coefficients depend on the position (x_{cen}, y_{cen}) of the reference axis. Fig. 7 shows the homogeneity curves for a displacement of the reference axis of +10 mm in x direction. The homogeneity curves as a function of x obtained from the modified harmonic spectrum are shifted by -10 mm with respect to the unshifted curve obtained directly from the field model, as it should. The curves as a function of y remain nearly unchanged.

Fig. 8 shows the same investigation, but with a displacement of the reference axis of 6mm in y direction with the expected result that the homogeneity curves obtained from the modified harmonic spectrum are shifted in y direction, but not in x direction.

The modified harmonic spectra thus describe the displacement of the reference axis correctly.

Fig. 9 shows the variation of the harmonic coefficients, multiplied with the phase factor $\cos(n\alpha_n)$, as a function of the position of the reference axis x_{cen} and y_{cen}.

5 Conclusion

A three dimensional field model was used to calculate the harmonic coefficients of the local field, the end field and the total field of the LEP Spectrometer Magnet. The numerical precision of the harmonic spectra is sufficient to describe the transverse homogeneity curves obtained directly from the field model with an accuracy of about 10 ppm. Harmonics up to order 6 have to be considered to achieve this accuracy. The scaling of the harmonic amplitudes with the reference radius corresponds to the theoretical expectation for not too small radii. A shift of the reference axis is described by the modified harmonic spectra.

References

[1] The LEP Spectrometer Project, LEP Spectrometer Working Group, CERN-SL note in preparation

[2] Magnetic field calculations for the LEP spectrometer project, M. Sassowsky, CERN SL-Note-99-011 MS

[3] Basic theory of magnets, A. Jain, CAS 1997 on Measurement and Alignment of Accelerator and Detector Magnets

[4] Technical specification for the supply of of the MBI dipole cores for LEP 200, CERN AT-MA/90-36

[5] Mésures magnetiques des aimants dipolaires d'injection du LEP 200, CERN AT-MA/CR/PV/fm-1403 Note technique 92-32

[6] Opera-3D version 7.005, Vector Fields Limited, 24 Bankside, Kidlington, Oxford OX5 1JE, England

[7] Opera-3D applications notes, VF-01-98-X6

[8] Opera-3D user guide, VF-01-98-D2

Distribution

R. Chritin (SL/MS)
D. Cornuet (SL/MS)
W. Kalbreier (SL/MS
P. Leclère (SL/MS)
G. Mugnai (SL/MS)
G. de Rijk (SL/MS)
B. Dehning (SL/BI)
M. Hildreth (SL/BI)
J. Palacios (EP/LE)
G. Wilkinson (EP/HC)
O. Pagano (LHC/MMS)

Appendix

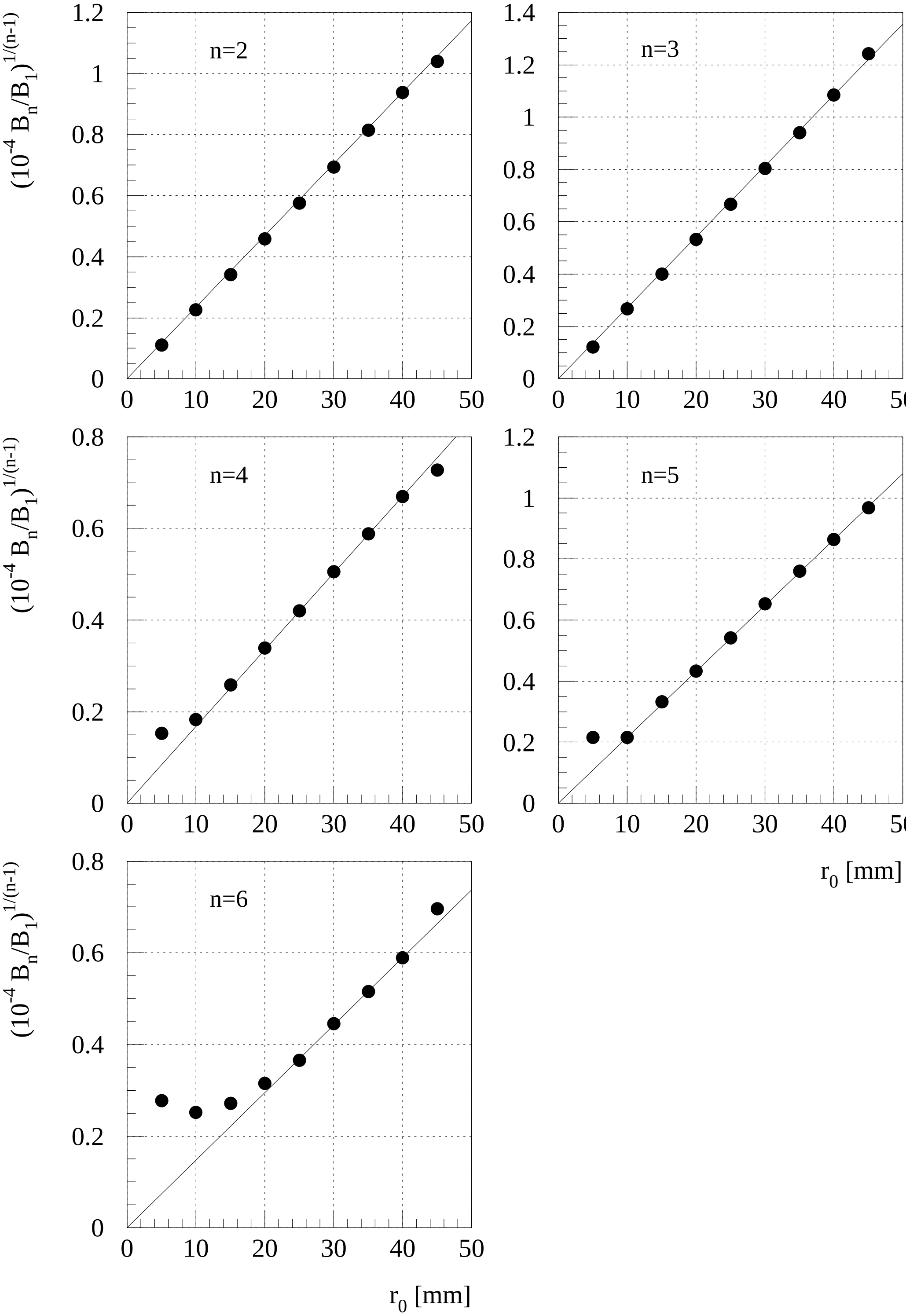

Figure 2: Variation of the harmonic amplitudes as a function of the reference radius

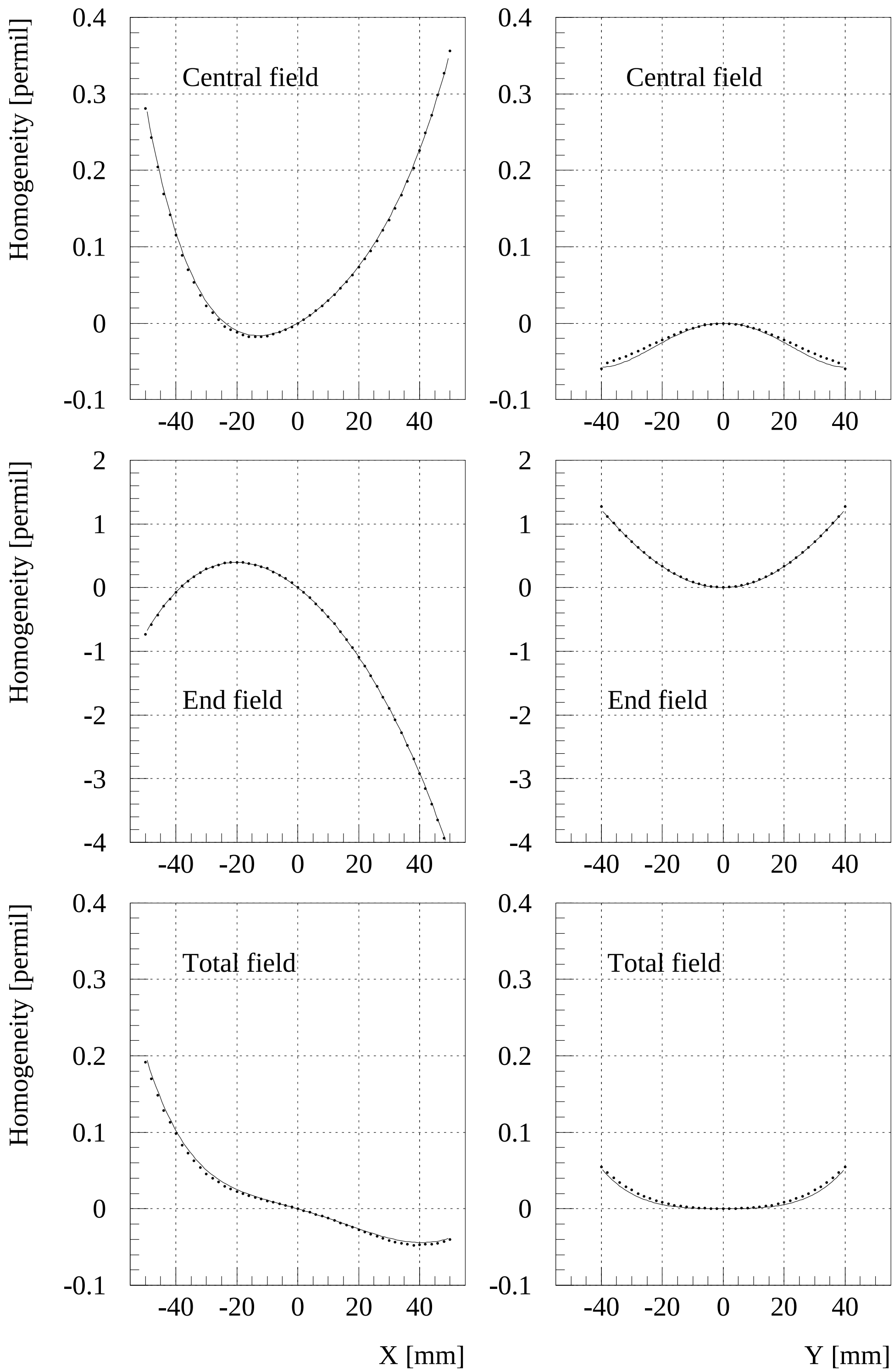

Figure 3: Homogeneity curves obtained indirectly from harmonic spectra (lines) and directly from the field model (points) at 100 GeV

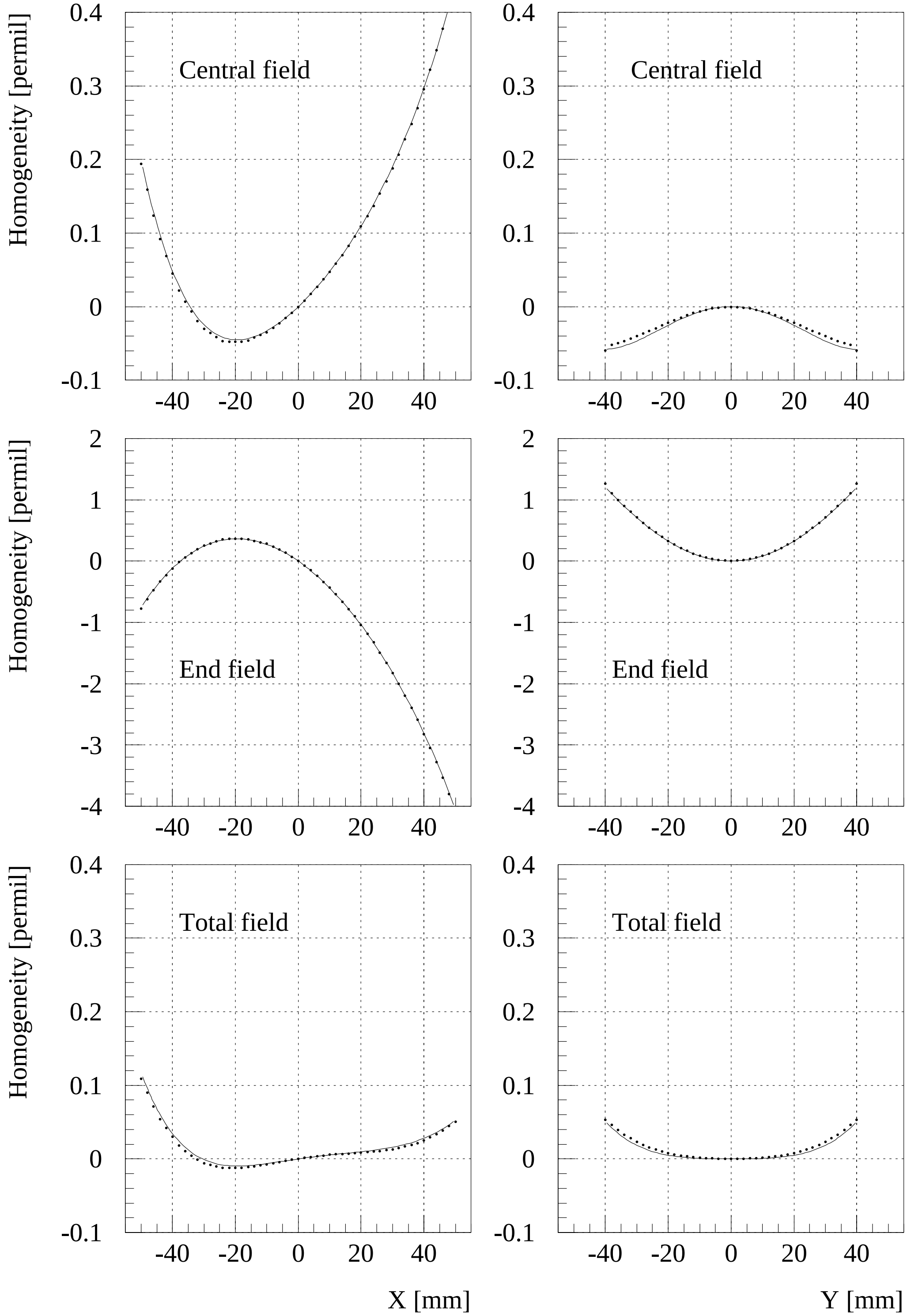

Figure 4: Homogeneity curves obtained indirectly from harmonic spectra (lines) and directly from the field model (points) at 44 GeV

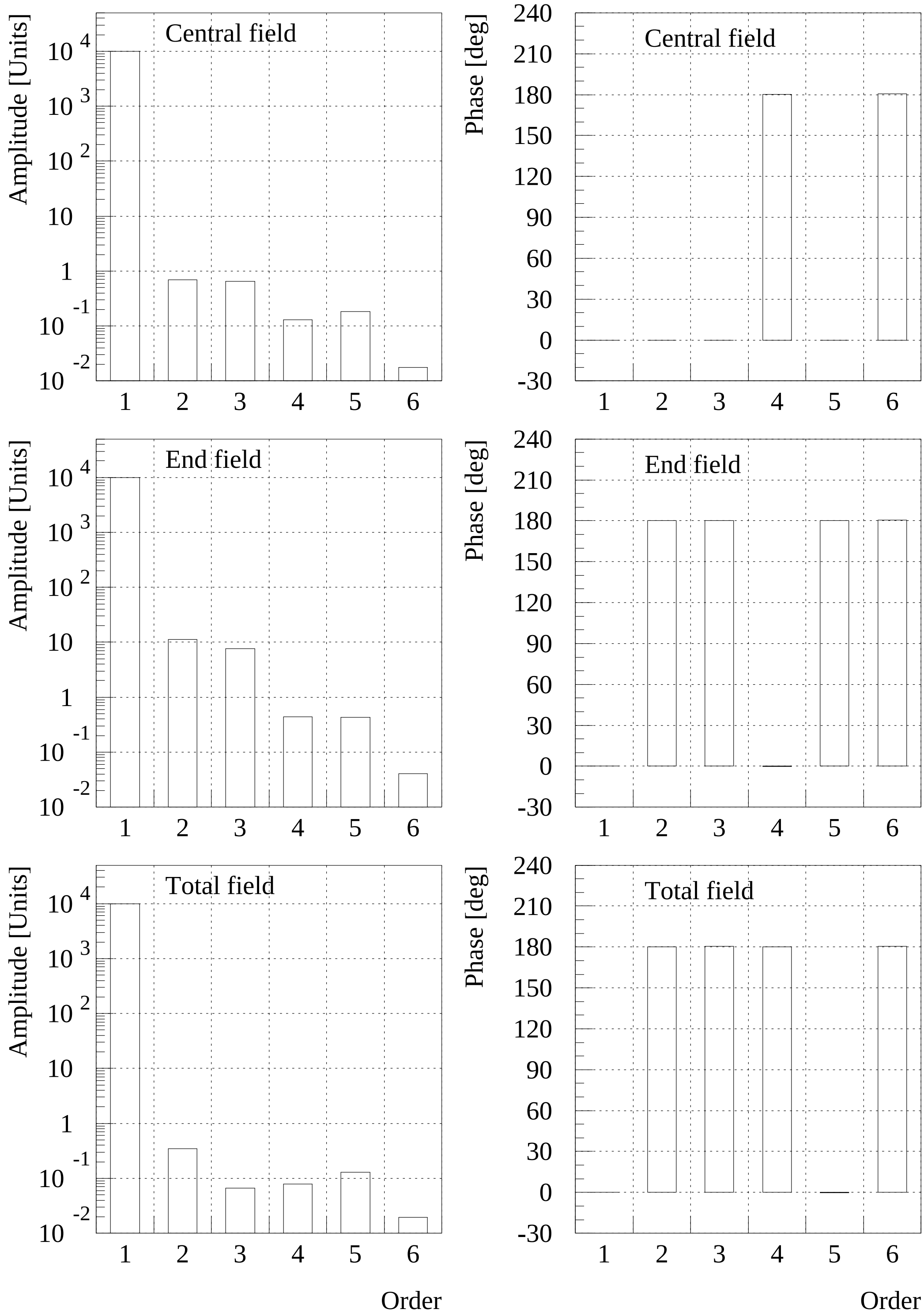

Figure 5: Harmonic spectra at 100 GeV

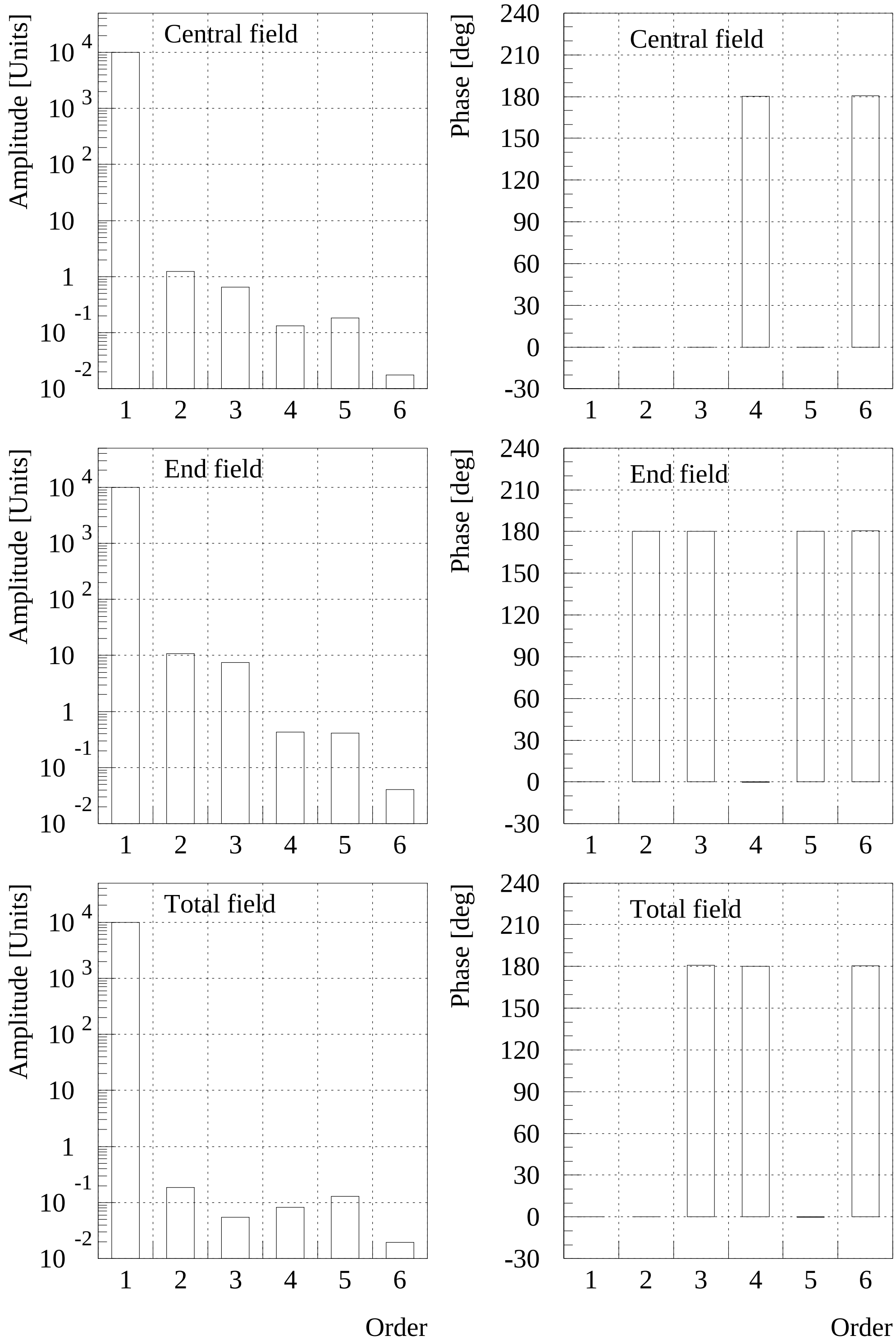

Figure 6: Harmonic spectra at 44 GeV

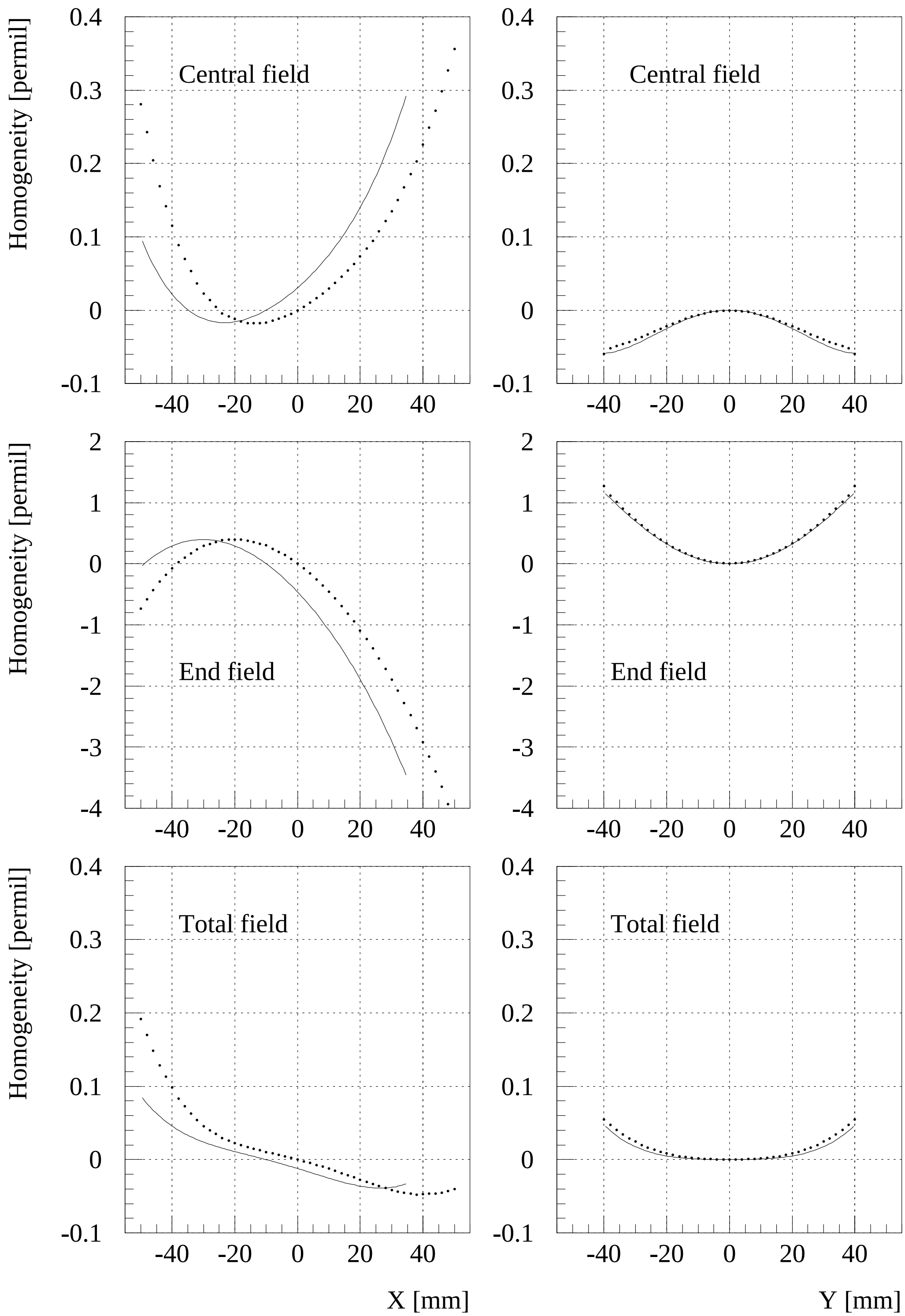

Figure 7: Homogeneity curves for a displacement of the reference axis in x direction

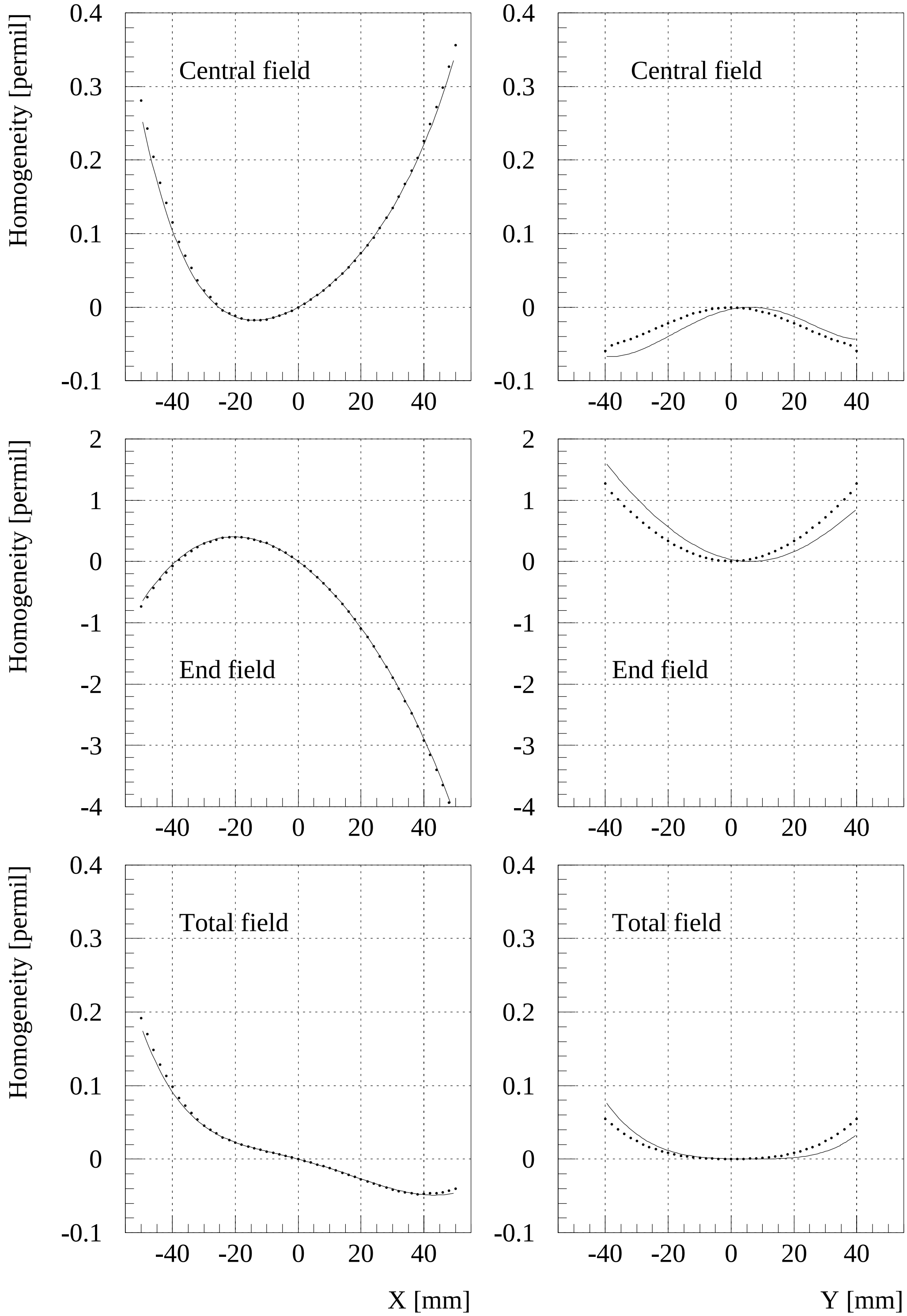

Figure 8: Homogeneity curves for a displacemt of the reference axis in y direction

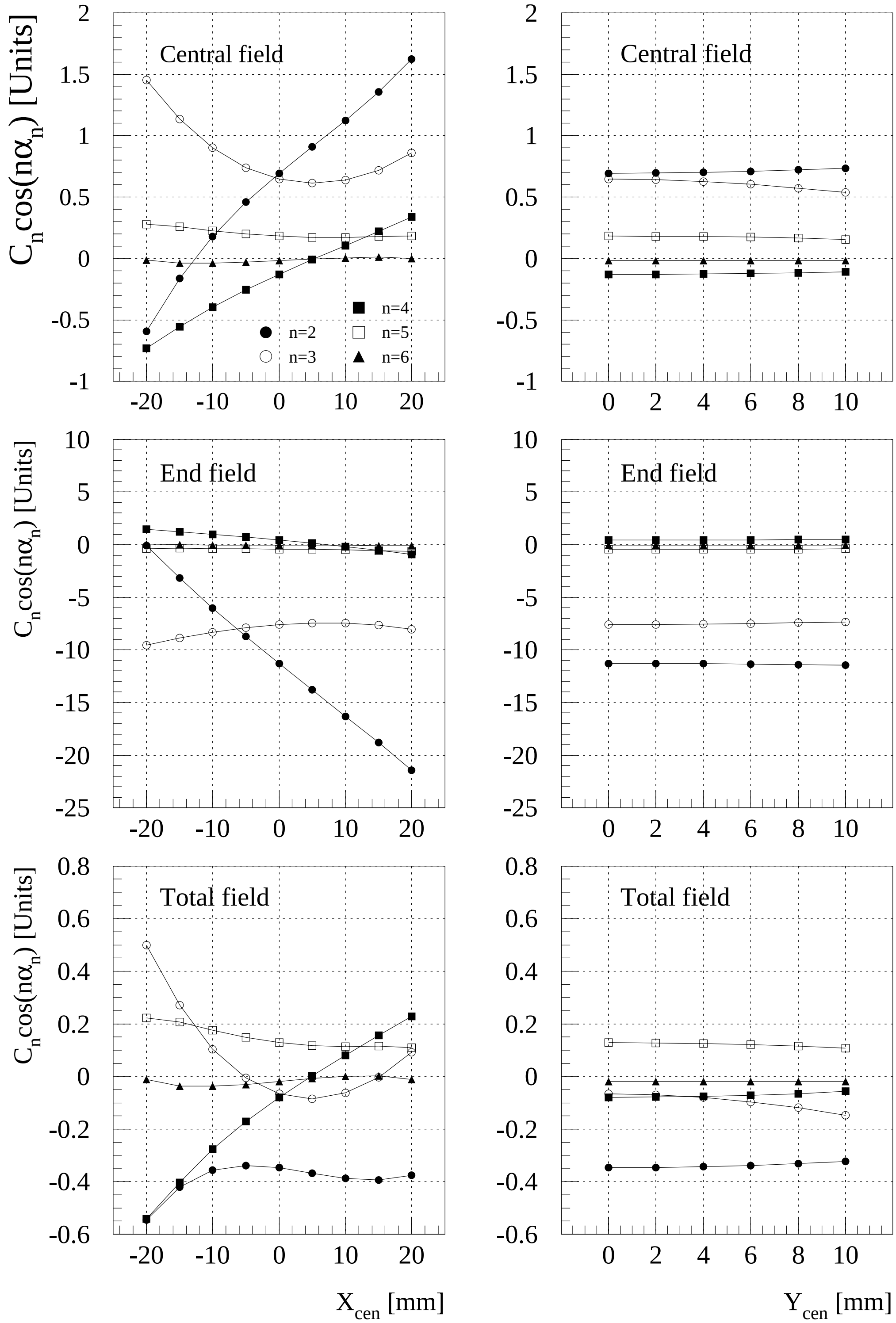

Figure 9: Variation of the harmonic coefficients as a function of the position of the reference axis